Computers and Concrete, *Vol. 21, No. 2 (2018) 117-126*
DOI: https://doi.org/10.12989/cac.2018.21.2.117

Behavior of reinforced lightweight aggregate concrete hollow-core slabs

Adel A. Al-Azzawi* and Basma M. Abdul Al-Aziz[a]

Department of Civil Engineering, Al-Nahrain University, Baghdad, Iraq

(Received February 4, 2017, Revised July 28, 2017, Accepted September 24, 2017)

Abstract. This research investigate the behavior of reinforced normal and lightweight aggregate concrete hollow core slabs with different core shapes, shear span to effective depth (*a/d*). The experimental work includes testing seven reinforced concrete slabs under two vertical line loads. The dimensions of slab specimens were (1.1 m) length, (0.6 m) width and (0.12 m) thickness. The maximum reduction in weight due to aggregate type was (19.28%) and due to cross section (square and circular) cores was (17.37 and 13.64%) respectively. The test results showed that the decrease of shear span to effective depth ratio from 2.9 to 1.9 for lightweight aggregate solid slab cause an increase in ultimate load by (29.06%) and increase in the deflection value at ultimate load or the ultimate deflection by (17.79%). The use of lightweight aggregate concrete in casting solid slabs give a reduction in weight by (19.28%) and in the first cracking and ultimate loads by (16.37%) and (5%) respectively for constant (*a/d*=2.9).The use of lightweight aggregate concrete in casting hollow circular core slabs with constant (*a/d*=2.9) (reduction in weight 32.92%) decrease the cracking and ultimate loads by (12%) and (5.18%) respectively with respect to the solid slab. These slab specimens were analyzed numerically by using the finite element computer program ANSYS. Good agreements in terms of behavior, cracking load (load at first visible crack) and ultimate load (maximum value of testing load) was obtained between finite element analysis and experimental test results.

Keywords: hollow core slabs; lightweight aggregate; reinforced concrete ; experimental tests; finite element analysis

1. Introduction

Structural lightweight concrete (SLWC) has successfully been utilized for long times in structural systems in buildings and bridges. In addition to its lighter weight, which lower dead loads, and thus decreases the costs of both superstructure and foundation, it has more resistance to fire and gives preferable heat and sound protection than concrete of normal density (Slate *et al.* 1986, Mays and Barner 1991). Lightweight concrete (LWC) is considered as having a density not exceeding 1920 kg/m^3, while normal density concrete is considered to have a usual density ranging between 2240 and 2480 kg/m^3 (ACI Committee 213R 2003). Hollow core slab (HCS) is precast, pre-stressed concrete slab with consistent voids extended throughout the length of the slab. This type of slab system shows a decrease in weight and, in this manner, cost and as a part of advantage, to utilize for insert electrical or mechanical runs. HCS likewise have an application in spandrel members, wall panels and bridge deck units (Stephen 2013).

Several researchers studied reinforced concrete slabs such as Sgambi *et al.* (2014) and Mousavi and Dehestani (2015) and gave indication on the behavior of such slabs.

Many studies around the world focus on reducing weight of slab by using lightweight aggregate or reducing the cross sectional area of slabs such as Hai-tao *et al*. (2011) examined the inner force transfer mechanism of a column-supported cast-in-situ hollow core slab using finite element analysis. The dimensions of the floor system were (21.6×21.6 m) consist from three panels in each direction, each panel (7200×7200 mm) with 300 mm thickness. The diameter of hole was 200 mm and tube filler's length was 900 mm with ribs having 100 mm width between holes. Both a hollow core slab and the corresponding solid slab were analyzed using ANSYS and the results were compared.

Rahman *et al*. (2012) tested full-scale pre-stressed precast hollow-core slabs with different shear span to depth (*a/d*), which were loaded to failure to ascertain the ultimate load-carrying capacity of these slabs. A total of 15 slab specimens, 5 and 2.5 m in span and having three different depths, 200, 250 and 300 mm were tested to failure using four-point load. The failure mode of hollow-core slabs was changed from pure flexure mode to flexure-shear mode for slabs with depth greater than 200 mm. The analysis of the experimental results showed that the existing ACI code equations underestimated the flexure-shear strength of these hollow-core slabs.

Brunesi *et al.* (2014) carried out comparison between experimental, analytical and finite element method for shear strength capacity of precast pre-stressed concrete hollow core slabs with (200-500) mm thick without transverse reinforcement through a nonlinear finite element analysis, which matched the experiments test data. These members (49specimens) characterized with six nominal slab depths, five hollow shapes with circular and non-circular voids, different voids ratios, several pre-stressing steel strands arrangements and levels of initial pre-stress then comparative

*Corresponding author, Assistant Professor
E-mail: dr_adel_azzawi@yahoo.com
[a]M.Sc. Student

http://www.techno-press.com/journals/cac&subpage=8
ISSN: 1598-8198 (Print), 1598-818X (Online)

Table 1 Properties of the tested slabs

Slab no.	Type and Description	Shear span to effective depth (*a*/*d*)	Core dimensions (mm)
1	Normal weight aggregate (NWA) solid slab	2.9	----
2	Lightweight aggregate (LWA) solid slab	2.9	----
3	Lightweight aggregate (LWA) solid slab	1.9	----
4	Lightweight aggregate hollow circular core slab (HCCS)	2.9	50 diameter
5	Normal weight aggregate hollow circular core slab (HCCS)	2.9	50 diameter
6	Lightweight aggregate hollow circular core slab (HCCS)	1.9	50 diameter
7	Lightweight aggregate hollow square core slab(HSCS)	1.9	50 side length

with traditional codes. From finite element (FE) results, the proposed numerical approach was validated by focusing on a single precast prestressed hollow-core unit, therefore the accuracy of the FE predictions obtained for nine specimens analyzed was quantified in comparison with experimental data.

Haruna (2014) studied the flexural behavior of precast pre-stressed concrete hollow-core units with cast-in-place concrete topping, through load testing of five full-scale specimens. The specimens were divided into two groups wide and narrow. Presence of cast-in-place topping slab improved the behavior of hollow-core units by increasing the flexural crack initiation and maximum load capacities as well as the stiffness. As a result of premature loss of composite behavior, the predicted load capacity of these specimens assuming a fully composite behavior remained on the non-conservative side. The obtained results suggested that the floor system made of cast-in-place concrete topping placed over the machine finished surface of precast concrete hollow-core units with no interfacial roughening is not able to provide the interface shear strength required to develop a fully composite behavior.

Lee *et al.* (2014) studied the web shear capacity of hollow core slabs (HCS) through a large number of shear tests. The analysis of results indicated that the minimum shear reinforcement requirement for deep HCS members are too severe, and that the web-shear strength equation in ACI 318 code does not provide good estimation of shear strengths for HCS members. Thus, a rational web-shear strength equation for HCS members was derived in a simple manner, which provides a consistent margin of safety on shear strength for the HCS members up to 500 mm deep. More shear test data would be required to apply the proposed shear strength equation for the HCS members over 500 mm in depth though.

AL-Azzawi and Abed (2017), investigated the behavior of moderately thick reinforced concrete slabs having hollow cores with various volumes and with different loading conditions by varying the (*a*/*d*) ratios. The experimental part included testing eight specimens of solid and hollow-core slab models having (2.05 m) length, (0.6 m) width and (25 cm) thickness under two monotonic line loads. Load versus deflection was recorded during test at mid span and under load. Numerically, the finite element method was used to study the behavior of these reinforced concrete slabs by using ANSYS computer program. The specimens of slab models were modeled by using (SOLID65) element to represent concrete slabs and (LINK180) element to represent the steel bars as discrete axial members between concrete nodes. The finite element analysis had showed good agreement with the experimental results with difference of (4.71%-8.68%) in ultimate loads. A parametric study was carried out by using ANSYS program to investigate the effects of concrete compressive strength, size and shape of core, type of applied load and effect of removing top steel reinforcement.

Based on previous studies, the reduction in weight due to both material and cross section has not yet been investigated. In the present research, two types of reduction in weight are achieved through using lightweight aggregate (LWA) and hollow cores (HC). The main objective of this study is to investigate the behavior of one way reinforced concrete slab with reduced weight experimentally and numerically.

2. Details of experimental test

The test specimens were seven reinforced concrete slabs tested under two vertical line loads. These slabs having a length of (1100) mm, width of (600) mm, thickness of (120) mm, reinforcement of (3Ø8 mm at long direction and 5Ø8 mm at short direction). The descriptions of the tested slabs are presented in Table 1, and Fig. 1. The abbreviation HCCS defines hollow circular core slab and abbreviation HSCS defines hollow square core slab.

For the slab specimens, the properties of the hardened concrete for the average of three samples and steel reinforcement which used for casting these slabs are summarized in Table 2.

3. Finite element model

A nonlinear finite element analysis has been carried out to analyze all tested solid and hollow-core slabs. The analysis was performed using ANSYS release (15.0) computer program (ANSYS User’s Manual 2013).

3.1 Element type

- SOLID65 element is used to model the concrete and it has eight nodes with three degrees of freedom at each node-translations in the nodal *x*, *y*, and *z* directions.
- LINK180 element is used to model steel reinforcement. This element is a 3D spar element and it

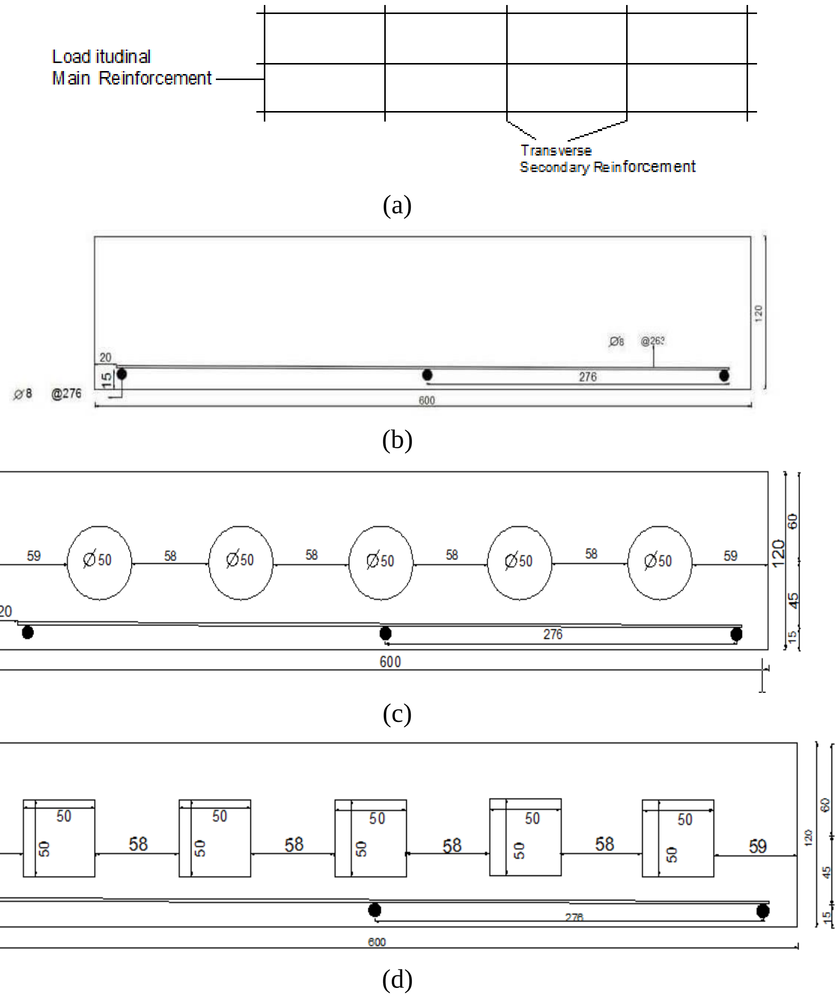

Fig. 1 (a) Specimens geometry and details, (b) Solid slab (c) and (d) Hollow core slabs (All dimensions are in mm)

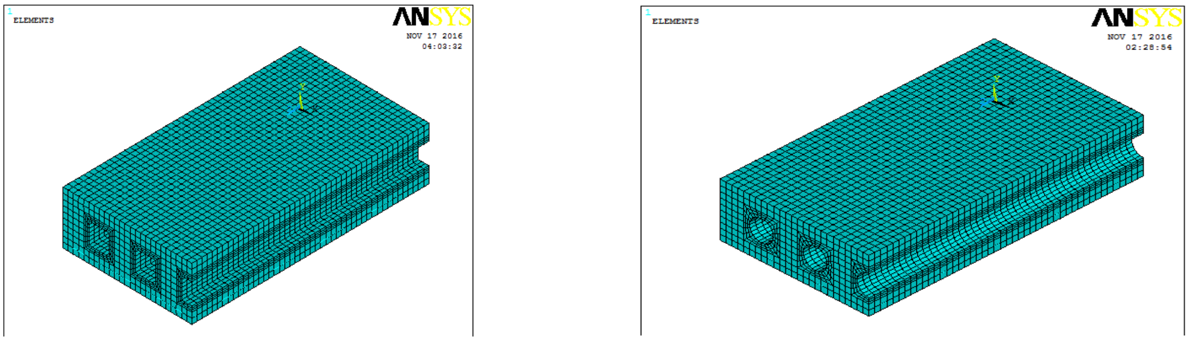

Fig. 2 Mesh of quarter of circular and square hollow core slab

has two nodes with three degrees of freedom-translations in the nodal *x*, *y*, and *z* directions. Perfect bond between the concrete and steel reinforcement is considered.

• SOLID185 element is an eight node solid element. It is used for modeling steel supports and rubber. The element is defined with eight nodes having three degrees of freedom at each node translations in *x*, *y* and *z* directions. Steel plates were added at support and point of loading locations in the finite element models (as in the actual slabs) to provide a more even stress distribution over the support and point of loading areas. The steel plates were assumed to be linear elastic materials.

• PLANE182 element was used for 2-D modeling of solid structures. It was used for the area plane around the circular shape of slab cores only.

3.2 Modeling and meshing stages

The dimensions of quarter model used in ANSYS program have (550 mm) length, (300 mm) width and (120

Table 2 Properties of materials

Properties of normal aggregate concrete material		
Property	Experimental	ACI318M (2014)
Dry density (γ_c) (kg/m^3)	2350	-
Compressive strength (f'_c) (MPa)	35.6	-
Splitting tensile strength(f'_{ct}) (MPa)	3.37	2.98 ($0.5\sqrt{f'_c}$)
Modulus of rapture (f_r) (MPa)	3.79	3.70 ($0.62\sqrt{f'_c}$)
Modulus of elasticity (E_c) (MPa)	28136	28043 ($4700\sqrt{f_c'}$) 29228 ($W_c^{1.5}0.043\sqrt{f_c'}$)
Properties of lightweight aggregate concrete material		
Dry density (γ_c) (kg/m^3)	1920	-
Compressive strength (f'_c) (MPa)	27.7	-
Splitting tensile strength(f'_{ct}) (MPa)	2.32	2.11 ($0.8*0.5\sqrt{f'_c}$)
Modulus of rapture (f_r) (MPa)	2.61	2.48 ($0.8*0.62\sqrt{f'_c}$)
Modulus of elasticity (E_c) (MPa)	19225	24736 ($4700\sqrt{f_c'}$) 19040 ($\gamma_c^{1.5}0.043\sqrt{f_c'}$)
Properties of steel reinforcement material		
Property	Test results	
Nominal diameter (mm)	8	
Calculated diameter (mm)	7.86	
Yield stress (f_y) (MPa)	578.18	
Ultimate stress (f_u) (MPa)	655.74	

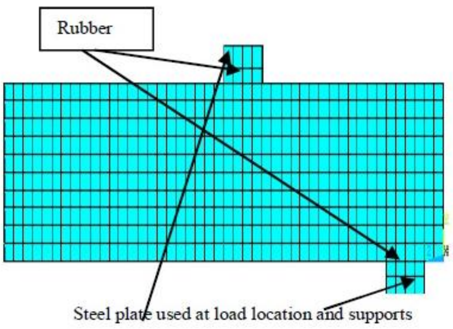

Fig. 3 Rubbers and steel plates for quarter of slab model that used in analysis

Table 3 Material properties for Solid185 element for modeling steel plates

	Parameter	Assumed value
Solid185	Modulus of elasticity (MPa)	2000000
	Poisson's ratio	0.3

Table 4 Material properties for Solid185 element for modeling rubber

	Parameter	Assumed value
Solid185	Modulus of elasticity (MPa)	6
	Poisson's ratio	0.3

mm) thickness are shown in Fig. 2. Seven specimens were analyzed by ANSYS program included solids slab (normal weight and lightweight concrete) with different *a/d* ratio (shear span to effective depth ratio), and hollow core slabs (normal weight and lightweight concrete) with different a\d ratio, and different core shapes additional to the experimental study parameters.

3.3 Loading and boundary condtions

In order to have realistic modeling, the cushion in ANSYS is modeled as two parts using the same element solid185. The first part represents rubber and second part represents steel plates. Two cushions of (10 mm) thickness were modeled using (Solid185) element to represent rubber, at the support, and two cushions at loading location. While two steel plates of (15 mm) thickness were formed utilizing (Solid185) element, are placed at the support and two steel plates at location of loading with same volume of concrete mesh (12 mm) in order to avoid stress concentration problems. This will provide a uniform stress distribution over the support area as shown in Fig. 3 for quarter of slab model. The properties of concrete and steel which are used in the analysis are based on the values given in Table 2. The propreties of steel plate and rubber used in the present study analysis are given in Tables 3 and 4.

4. Experimental and numerical results

Experimental work and finite element analysis results which are obtained are presented and then discussed. Experimental measurements which are carried out by testing seven slabs including the ultimate loads, load-deflection curves are given. Comparisons between the experimental and the numerical results are made to verify the application of the suggested numerical idealization on the tested slabs. ANSYS program was used to analyze the same slabs and study the effect of some additional parameters on the behavior of these slabs.

4.1 Loads and deflections at failure

The experimental test results and description of samples are given in Table 5.

Table 5 Description and test results of samples

Slab no.	Description of samples	Weight reduction (%)	*a/d*	First cracking load Pcr (kN)	Deflection at cracking load (mm)	Ultimate load Pu (kN)	Deflection at ultimate load (mm)	Mode of failure	(P_{cr}/P_u) (%)
1	NWA solid slab	0	2.9	30	2.20	75.6	31.41	Flexural	39.68
2	LWA solid slab	19.28	2.9	25	2.26	71.82	35.35	Flexural	34.81
3	LWA solid slab	19.28	1.9	35	3.3	101.25	43.0	Shear-Flexural	34.57
4	LWA HCCS	32.92	2.9	22	3.2	68.1	38.52	Flexural	32.31
5	NWA HCCS	13.64	2.9	28	3.65	71.45	33.6	Flexural	39.19
6	LWA HCCS	32.92	1.9	33	3.34	97.12	46.6	Shear-Flexural	33.98
7	LWA HSCS	36.65	1.9	30	3.5	73.21	12.35	Shear	40.98

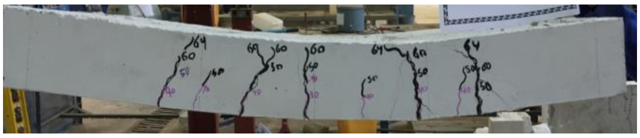

Fig. 4 Crack pattern at ultimate load for slab no.1

Fig. 5 Crack pattern at ultimate load for slab no. 2

Fig. 6 Crack pattern at ultimate load for slab no. 3

Fig. 7 Crack pattern at ultimate load for slab no. 4

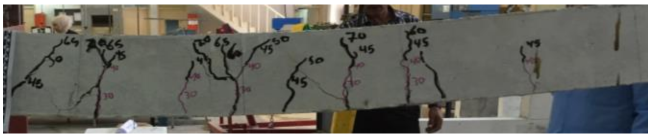

Fig. 8 Crack pattern at ultimate load for slab no. 5

Fig. 9 Crack pattern at ultimate load for slab no. 6

Fig. 10 Crack pattern at ultimate load for slab no.7

For normal weight aggregate solid slab, cracks are developed at about (39.68%) of the ultimate load while for lightweight aggregate solid slabs cracks are developed earlier at about (34.81%) of the ultimate load with same *a/d* ratio. This is may be due to the difference in compressive strength between normal and lightweight aggregate used mixes. For lightweight aggregate solid slabs cracks are developed at about (34.57-34.81%) of the ultimate load with different *a/d* ratio. For hollow circular core slab made with normal aggregate, cracks are developed at about (39.19%) of the ultimate load while lightweight aggregate hollow circular core slab cracks are developed at about (32.31%) of the ultimate load with same *a/d* ratio. This is also due to the difference in compressive strength between normal and lightweight aggregate used mixes. For lightweight aggregate hollow circular core slabs cracks are developed at about (32.31-33.98%) of the ultimate load with different *a/d* ratio. For lightweight aggregate hollow core slabs cracks with different core shapes (circular and square). Cracks are developed at about (33.98-40.98%) of the ultimate load with same *a/d* ratio. The reason for that may be due to different core shape and mode of failure. It was noticed that shear cracks appeared in slabs which was tested with (*a/d*) ratios (1.9) especially in hollow core slab due to position of applied loads and presence the holes but the failure of these slabs were shear flexural failure except slab no. 7 which was in shear mode. The crack patterns for the tested slabs are shown in the Figs. 4 to 10.

A comparison between the ultimate loads of the experimentally tested slabs and the final loads obtained from finite element models is shown in Table 6. The final loads for the finite element models are the last applied loads before the solution starts to diverge due to numerous cracks and large deflection in Y-direction (UY). The ultimate loads obtained from numerical models are in good agreement with the corresponding values from the experimentally tested slabs with average difference of 7%. The numerical results show greater ultimate load with smaller deflection at the ultimate load stage as compared to experimentally results.

Table 6 Results of experimental work and finite element analysis

Slab no.	Description of samples	Shear span to effective depth (a/d) ratio	Ultimate load P_u (kN) in experimental work.	Ultimate load P_u (kN) by ANSYS	Difference %	Mid span deflection Δ_u (mm) in experimental work	Mid span deflection Δ_u (mm) by ANSYS	Difference %
1	NWA solid slab	2.90	75.60	80.60	6.61	31.41	28.48	-9.33
2	LWA solid slab	2.90	71.82	77.60	8.05	35.35	32.77	-7.29
3	LWA solid slab	1.90	101.25	109.20	7.85	43.00	39.84	-7.34
4	LWA HCCS	2.90	68.10	75.25	10.50	38.52	38.44	-0.21
5	NWA HCCS	2.90	71.45	76.40	6.93	33.60	31.02	-7.66
6	LWA HCCS	2.90	97.12	106.76	9.93	46.60	43.83	-5.94
7	LWA HSCS	1.90	73.21	71.00	3.02	12.35	\10.73	-13.08
		Average difference			7.56			7.26

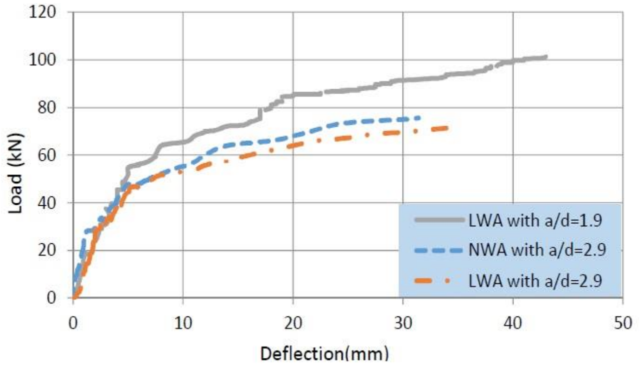

Fig. 11 Load-deflection relationship of solid slabs for different a/d ratios

4.2 Load-deflection curves

For solid slabs, the test results show that the decrease of shear span to effective depth ratio (*a/d*) for lightweight aggregate solid slab cause an increase in ultimate load (maximum value of testing load) and the failure mode became shear. This is may be due to the decrease in applied moments. The decreasing of (*a/d*) ratio from 2.9 to 1.9 produce an increase in cracking load by (28.57%) and ultimate load by (29.06%). The test results show also that using lightweight aggregate instead of normal weight aggregate in solid slabs with the same *a/d* ratio give a reduction in weight by (19.28%) and in first cracking and ultimate loads by (16.67%) and (5%) respectively as shown in Fig. 11.

The normal weight aggregate solid slabs with a/d ratio equal to 2.9 show an increase in cracking and ultimate loads by (6.68%) and (5.49%) respectively with respect to the hollow core slabs (reduction in weight due to cross section is 13.64%) with same aggregate type as shown in Fig. 12. But the deflection at ultimate load is decreased by (6.97%) for solid slab. The flexural mode of failure is obtained for both slabs with more spread cracks for the hollow circular core slab.

The lightweight aggregate solid slabs with *a/d* ratio equal to 2.9 (reduction in weight due to aggregate type is

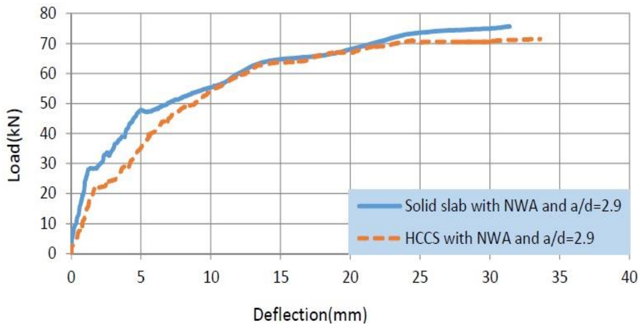

Fig. 12 Load-deflection relationship of solid and hollow circular core slabs

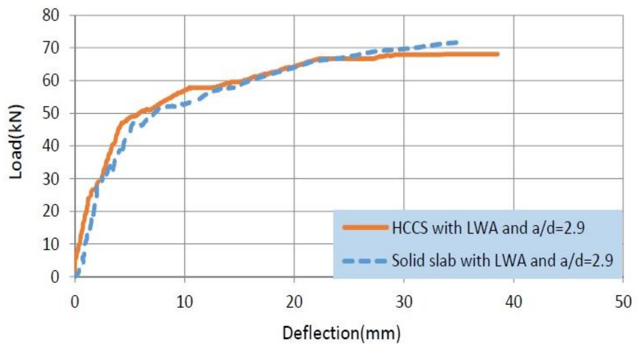

Fig. 13 Load-deflection relationship of solid and hollow circular core slabs

19.28%) show an increase in first cracking and ultimate loads by (12%) and (5.18%) respectively with respect to hollow circular core slabs (reduction in weight due to cross section and aggregate type is 32.92%) as shown in Fig. 13. But the deflection at ultimate load is decreased by (8.97%) with flexural mode of failure for both slabs.

For lightweight aggregate slabs with *a/d* ratio equal to 1.9, the hollow square core slabs shows reduction in first cracking and ultimate loads by (14.29%) and (27.70%) respectively compared to solid slabs.

The shear mode of failure was recognized for the hollow square core slabs (reduction in weight due to cross section and aggregate type is 36.64%).

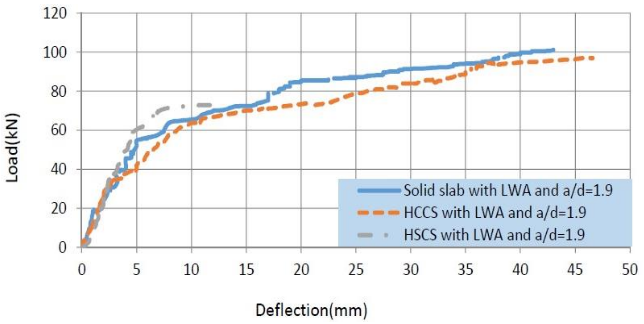

Fig. 14 Load-deflection relationship of solid and hollow core slabs

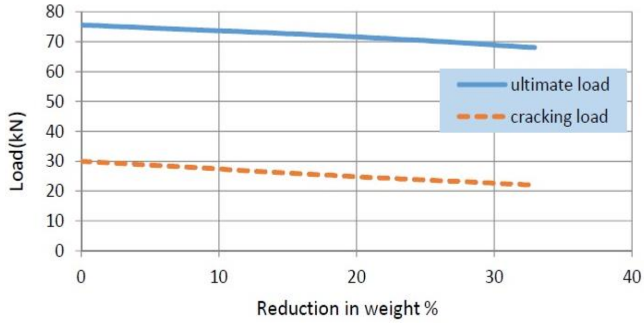

Fig. 17 Relationship between reduction in weight and applied loads (cracking and ultimate loads)

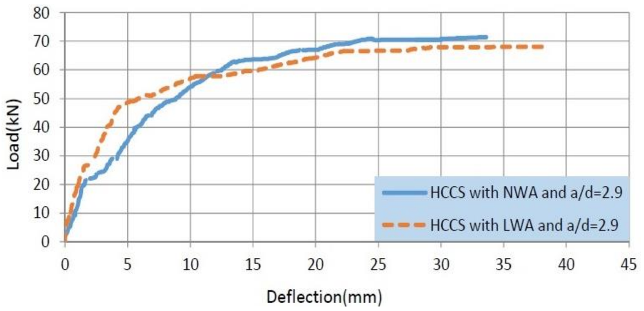

Fig. 15 Load-deflection relationship of normal and lightweight concrete hollow core slabs

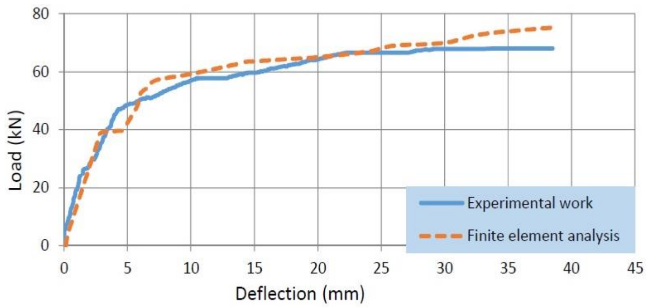

Fig. 18 Experimental and finite element load - deflection curves for slab no.4

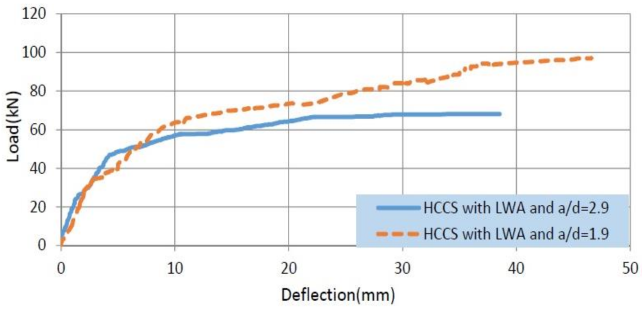

Fig. 16 Load-deflection relationship of hollow core slabs with different in a/d ratios

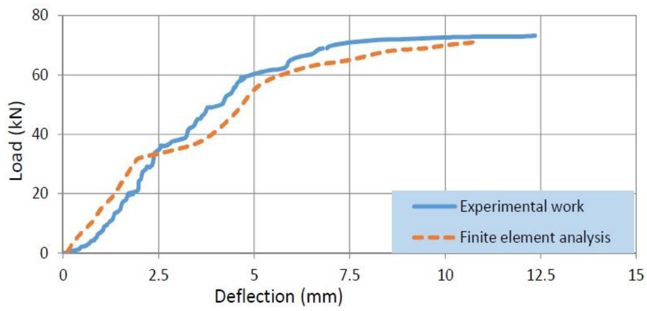

Fig. 19 Experimental and finite element load - deflection curves for slab no.7

The hollow circular core slab (reduction in weight is 32.92%) shows an increase in first cracking and ultimate loads by (9%) and (24.6%) respectively compared to hollow square core slab as shown in Fig. 14. The shear failure mode is obtained for hollow square core slab while shear flexural failure is obtained for circular core.

For hollow circular core slab with *a/d* equal to 2.9 and has a reduction in cross section by (13.64%) show higher cracking and ultimate loads than same slabs with lightweight aggregate which gives a total reduction in weight by (32.92%). The increase in cracking and ultimate loads was (21.43%) and (4.69%) respectively as shown in Fig. 15. The type of aggregate does not have effect on mode of failure but it effects on the spread of cracks and the nature of crack surface.

For lightweight aggregate hollow circular core slabs having different in *a/d* ratio (1.9 and 2.9) with reduction in weight of (32.92%) show a reduction in first cracking and ultimate loads with increasing *a/d*. For *a/d* increased from 1.9 to 2.9, the reduction in first cracking and ultimate loads was (33.33% and 29.88%) respectively. Also, the deflection is decreased by (17.34%) as shown in Fig. 16.

The cracking and ultimate load versus reduction in weight shown in Fig. 17. It can be noted that the ultimate and cracking loads decreased with reducing slab weight.

The deflection (vertical displacement) in *Y*- direction (UY) is obtained at the center of mid span and under the load (the bottom face of the slab). The load versus deflection plots obtained from the numerical and the experimental studies are presented for comparison in Figs. 18 and 19. The load-deflection curves of slabs show good correspond with the experimental test result. Results of comparison between experimental work and numerical analysis are in the range (3.05-10.5%) in ultimate load and (0.21-13.08) % in ultimate deflection value.

Deflection contours obtained from finite element analysis are shown in Figs. 20 and 21. It is obvious that all slabs with shear span to effective depth ratio equal to 2.9 have similar general behavior with smaller difference in the value of maximum deflection. For the shear span to

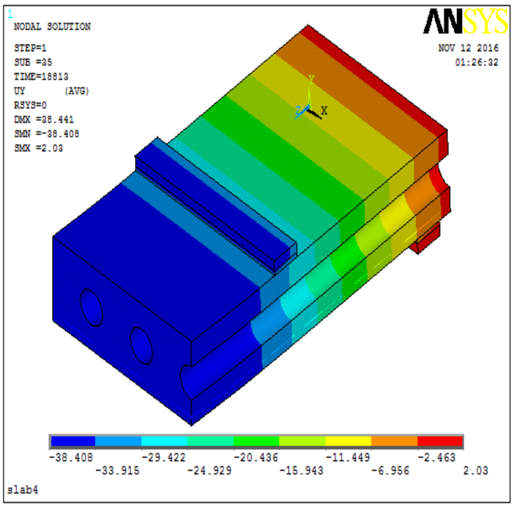

Fig. 20 Deflection contours in y-direction of tested slab no.4 at ultimate load

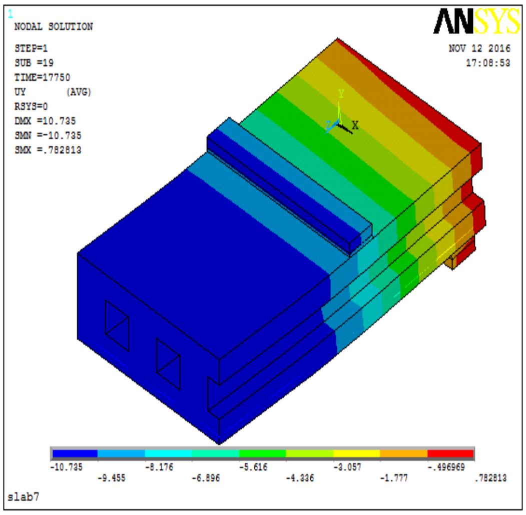

Fig. 21 Deflection contours in y-direction of tested slab no.7 at ultimate load

effective depth ratio equal to 1.9 the slab no.7 show different behavior because the mode of failure is different (hollow square core slab).

4.3 Crack pattern

As expected, the main cracks for most tested slabs commenced at middle third (flexural cracks) from the bottom face as a line with the width of the slab and the slabs exhibited ductile flexural failure and in some cases shear failure. It was noted that some of shear cracks appeared in slabs which tested with (*a/d*) ratios (1.9 and 2.9) especially in hollow-core slab due to position of applied loads and the presence of the holes (hollow-core slab) but these slabs are failed in flexure. ANSYS computer program displays circles at locations of cracking or crushing in concrete elements. Figs. 22 and 23 show the location of cracks from experimental test and finite element analysis along the hollow-core slabs.

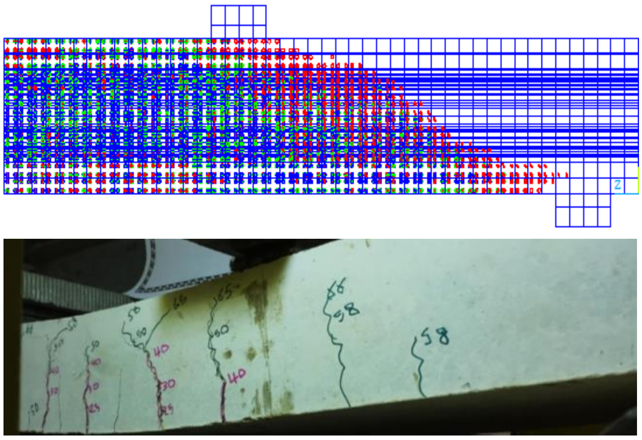

Fig. 22 Crack pattern at ultimate load for slab no.4

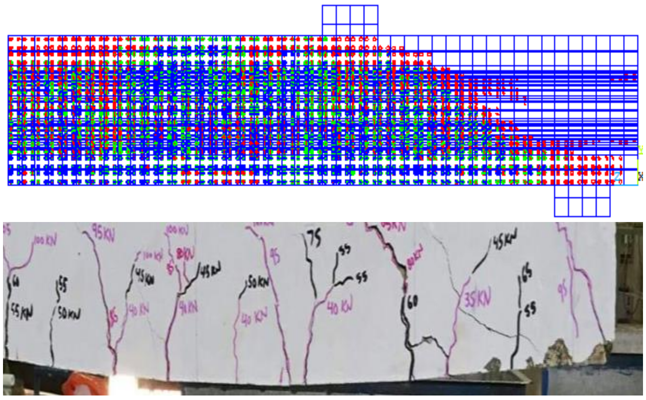

Fig. 23 Crack pattern at ultimate load for slab no. 5

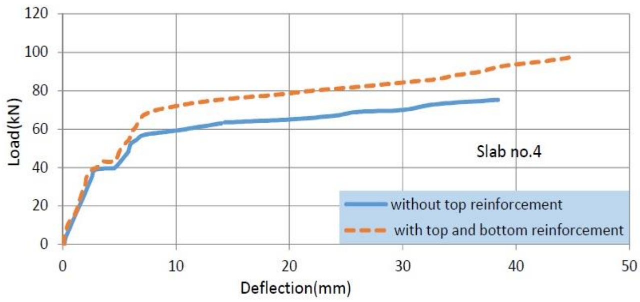

Fig. 24 Effect of top reinforcement layer on the behavior of lightweight aggregate hollow circular core slab

4.4 Parametric study

4.4.1 Effect of top reinforcement layer

Fig. 24 shows the effect of using top and bottom steel reinforcement. Slab no.4 is hollow circular core slab made with lightweight aggregate and core diameter (50 m) under two line loads with *a/d* equal (2.9) was analyzed first with only bottom reinforcement and then analyzed with top and bottom reinforcement with the same characteristic (bars diameter=8 mm and yield stress=548 MPa). It was noted that the ultimate load and deflection values of the slab is increased by about 29.37% and 16.15% respectively for slab with top reinforcement (also it has flexural failure mode). This is may be due to the existence of top reinforcement will distribute the stresses around the core

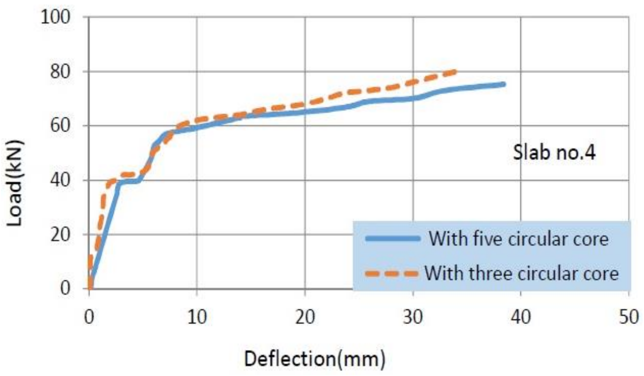

Fig. 25 Effect of number of cores on the behavior of lightweight aggregate hollow circular core slab

and prevent crushing of the concrete over the cores due to the increase in stresses.

4.4.2 Effect of number of cores

Slab4 (HCCS with LWA, *a/d*=2.9 and reduction in weight about 32.92%) is utilized to study the effect number of core on the load-deflection response. Slab no. 4 was analyzed first with five cores and then the same slab is analyzed with only three cores. The load deflection curves for this slab are shown in Fig. 25. It is found that the load-deflection behavior of slab with three cores is stiffer than those with five cores. The ultimate capacity was found to be greater for slabs with three cores than those with five cores by about 8.97% and also the deflection value is decreased when using three cores by about 10.77% but the reduction in weight decreased to become about 27.46% and it has flexural mode of failure.

5. Conclusions

Based on the results of this research, the following conclusions can be drawn:

• Two types of reduction in weight can be obtained for a slab. The first is by using lightweight aggregate concrete and the second is by using hollow core (reduce cross-sectional area). In this study the maximum reduction in weight due to aggregate type was (19.28%) and due to cross section was (17.365%). The crushed bricks can be satisfactory used as a lightweight coarse aggregate for making structural lightweight concrete with acceptable strength of 27.7 MPa.

• It is found that the decrease of shear span to effective depth ratio for lightweight aggregate solid slab cause an increase in cracking load by (28.57%) and in ultimate load by (29.06%). The mode of failure change from flexural to shear flexural.

• The use of lightweight aggregate concrete in casting solid slabs give a reduction in weight by (19.28%) and in cracking and ultimate loads by (16.37%) and (5%) respectively for constant (*a/d*=2.9).

• The use of lightweight aggregate concrete in casting hollow circular core slabs with constant (*a/d*=2.9) (reduction in weight 32.92%) give a decrease in the cracking and ultimate loads by (12%) and (5.18%) respectively with respect to solid slab of same aggregate type. The flexural mode of failure is obtained for both slabs.

• The use of lightweight aggregate concrete in casting hollow square core slabs with constant (*a/d*=1.9) (reduction in weight 36.64%) give a decrease in the cracking and ultimate loads by (14.29%) and (27.70%) respectively compared to the solid slab of same aggregate type. The failure mode changes from shear-flexural failure to shear failure.

• For (*a/d*=1.9), the hollow circular core slab shows an increase in cracking and ultimate loads by (9%) and (24.6%) respectively compared to hollow square core slab. The shear mode of failure is obtained for square core slab while shear flexure mode of failure is obtained for circular core slab.

• The use of lightweight aggregate concrete in casting hollow circular core slab with (*a/d*=2.9) (reduction in weight by 32.92%) show lesser cracking and ultimate loads of (21.43%) and (4.69%)

• The ultimate loads obtained from finite elements are in good agreement with experimental results with (7.56%) difference. The difference in ultimate deflection was (7.26%).

• The crack patterns obtained from finite elements are in good agreement with experimental ones.

• The effect of using top reinforcement for hollow circular core slab (*a/d*=2.9) is found to be significant. It was noted that the ultimate load and deflection increased by (29.37%) and (16.15%) respectively.

• The effect of number of cores is found to be significant for hollow circular core slab (*a/d*=2.9). If the number of cores increased from 3 to 5 the ultimate load decreased by (8.97%) and the deflection is increased by (10.77%). The reduction in weight increased from (27.46%) to (32.92%).

References

ACI 213R-03 (2003), Guide for Structural Lightweight-Aggregate Concrete, American Concrete Institute, Detroit, U.S.A.

ACI318-14 (2014), Building Code Requirements for Structural Concrete and Commentary, American Concrete Institute, Detroit, U.S.A.

Al-Azzawi, A.A. and Abed, S.A. (2017), “Investigation of the behavior of reinforced concrete hollow-core thick slabs”, *Comput. Concrete*, **19**(5), 567-577.

ANSYS 15.0 Inc. (2013), ANSYS User’s Manual, SAS IP, Inc., Version 15.0, U.S.A.

Brunesi, E., Bolognini, D. and Nascimbene, R. (2014), “Evaluation of the shear of precast-prestressed hollow core slab: Numerical and experimental comparison”, *Mater. Struct.*, **48**(5), 1503-1521.

Hai-Tao, L., Deeks, A., Liu, L., Huang, D. and Su, X. (2011), “Moment transfer factors for column-supported cast-in-situ hollow core slabs”, *J. Zhejiang Univ.*, **13**(3), 165-173.

Haruna, S.I. (2014), “Flexural behavior of precast pre-stressed concrete hollow core slabs with cast-in-place concrete topping”, M.S. Dissertation, Atılım University, Turkey.

Lee, D.H., Park, M., Oh, J., Kim, K.S., Im, J. and Seo, S. (2014), “Web-shear capacity of prestressed hollow core slab unit with

consideration on the minimum shear reinforcement requirement", *Comput. Concrete*, **14**(3), 211-231.
Mays, G.C. and Barner, R.A. (1991), "The performance of lightweight aggregate concrete structures in service", *Struct. Eng.*, **69**(20), 351-360.
Mousavi, S.S. and Dehestani, M. (2015), "Implementation of bond-slip effects on behavior of slabs in structures", *Comput. Concrete*, **16**(2), 311-327.
Rahman, M.K., Baluch, M.H., Said, M.K. and Shazali, M.A. (2012), "Flexural and shear strength of pre-stressed precast hollow-core slabs", *Arab. J. Sci. Eng.*, **37**(2), 443-455.
Sgambi, L., Gkoumas, K. and Bontempi, F. (2014), "Genetic algorithm optimization of precast hollow core slabs", *Comput. Concrete*, **13**(3), 389-409.
Slate, F.O., Nilson, A.H. and Martinez. (1986), "Mechanical properties of high-strength lightweight concrete", *ACI J.*, **83**(4), 606-613.
Stephen, C. (2013), "Hollow core manufacturing and factory design", *Ind. Concrete J.*, 20-25.

AW